

REQUIRED STRENGTH FOR PROBABILISTIC SEISMIC DESIGN AND  
DAMAGE ASSESSMENT OF REINFORCED CONCRETE STRUCTURES

by  
Masaya Murakami<sup>I</sup>

SUMMARY

Nonlinear response analyses of single degree of freedom structural systems were carried out in probabilistic terms by using a family of twenty artificial earthquake accelerograms. In order to simulate wall-frame reinforced concrete buildings, the structural systems were composed of a parallel combination of origin-oriented hysteretic models and degrading trilinear hysteretic models which fail primarily in shear and flexure, respectively. The stiffness properties of each model were varied in terms of displacement and strength at cracking and yielding. Selected results obtained in the overall investigation are presented and their application are discussed compared with the independent results of each model.

INTRODUCTION

A criterion of seismic resistant design is to provide buildings with strength and ductility so that response displacement does not exceed the displacement capacity during an earthquake. Performance and damage assessment of buildings is carried out by estimating their strength and ductility capacities considering the intensity of earthquake ground motions. If the characteristics of ground motions and hysteretic models are not changed, and the peak acceleration level and the strength level alone are assumed variables, the peak acceleration, strength and ductility factor are connected with each other so that one of them is obtained by determining the others on nonlinear response analysis for the single degree of freedom system. The strength level normalized by the product of the mass and peak acceleration is called the required strength ratio of a ductility factor.

In general, reinforced concrete buildings are composed of various types of framing system such as shear walls, short columns, and ductile walls and frames. The purpose of the present paper is to discuss how strength and ductility of each framing system have influence on the seismic capacities of the overall system by computing nonlinear response for idealized models, and to produce basic data to approach to more reliable estimation of the earthquake resistant capacities of wall-frame reinforced concrete buildings.

The required strength ratios had been independently obtained in probabilistic terms for an origin-oriented hysteretic model and four degrading trilinear hysteretic models subjected to five types of artificial earthquake accelerograms, the former representing the behaviour of a structural wall and short column failing in shear, and the latter simulating the flexural behaviour of a frame structure [1]. In this investigation are adopted idealized structural systems which are composed of a parallel combination of each of three origin-oriented models containing the above-mentioned model and one of the four degrading trilinear models to simulate wall-frame reinforced concrete

---

I Professor, Faculty of Engineering, Chiba University

buildings in the similar manner as the paper [2]. Since it was the intent of this investigation to concentrate on low-rise reinforced concrete buildings, nonlinear response analyses of single degree freedom structural systems were carried out in probabilistic terms by using a family of twenty artificial earthquake accelerograms equal to one of the five types. The stiffness properties of both models were varied in terms of displacement and strength at cracking and yielding. By using resulting response ductility factors were finally obtained the interaction curves between required strength levels of both models for various levels of ductility factors.

#### ARTIFICIAL EARTHQUAKE ACCELEROGRAMS

Since the required strength ratios of the four types (Types A, B, C, D) had been quite close each other, one of them was selected in this investigation, namely, Type B which represented that class of ground motion containing the N-S component of acceleration recorded during the 1940 El Centro, California, earthquake [1,3]. The characteristics of Type B are shown in Fig. 1 in terms of response acceleration ratios for linear model at four probability distribution levels following the method of the paper [4]. The response acceleration spectra suggest that Type B has the characteristic period in the neighborhood of 0.4 sec. The required strength ratios of Type B for  $\mu_{85}$  are shown in Figs. 2 and 3, where  $\mu_{85}$  is a ductility factor at the 85% probability distribution level. Note that required strength levels decrease, and the period corresponding to their peak levels becomes shorter, as ductility factor is larger as shown in Figs. 1 through 3, and that required strength levels decrease as period is longer as shown in Figs. 2 and 3.

#### STRUCTURAL MODELS

The single degree of freedom structural system shown in Fig. 4 is used in this investigation as the basic form for a parallel combination of two hysteretic models. The stiffness properties  $K_S$  and  $K_B$  are represented by three origin-oriented hysteretic models and a degrading trilinear hysteretic model, respectively. The overall hysteretic models are classified into three cases, namely, Case I, II and III depending on the characteristics of three origin-oriented models.

##### Origin-Oriented Hysteretic Model

This model is shown in Fig. 5 where its original skeleton curve is a trilinear shape with stiffness changes at shear cracking point ( $Q_{sc}, \delta_{sc}$ ) and shear yielding point ( $Q_{sy}, \delta_{sy}$ ) [5]. Reduction of loads follows linear path always directed through the origin, e.g. path A'O and A''O in Fig. 5 and reduces the stiffness  $K_1$ . The model plotted in Fig. 5 is for  $Q_{sy} = 1.9 Q_{sc}$  and  $\delta_{sy} = 10.0 \delta_{sc}$  corresponding to Case I and II, but the stiffness  $K_3$  is negative in Case II. The model in Case I is all the same as that of the paper [1]. The model in Case III are characterized by  $Q_{sy} = 3.0 Q_{sc}$  and  $\delta_{sy} = 6.0 \delta_{sc}$  equal to those of the degrading trilinear model as stated later.

##### Degrading Trilinear Model

This model is shown in Fig. 6 where its original skeleton curve is

also a trilinear shape with stiffness changes at flexural cracking point ( $Q_{bc}$ ,  $\delta_{bc}$ ) and flexural yielding point ( $Q_{by}$ ,  $\delta_{by}$ ) [5]. Up to yielding, the model behaves exactly like the standard bilinear model having stiffnesses  $K_1$  and  $K_2$ . In a case where displacement exceeds the yielding displacement, maximum displacement is treated as a new yielding point, e.g. point C in Fig. 6, and the stiffnesses  $K_1$  and  $K_2$  are reduced to  $\alpha K_1$  and  $\alpha K_2$ , respectively. The Fig. 6 is for  $Q_{by} = 3.0 Q_{bc}$  and  $\delta_{by} = 6.0 \delta_{bc}$  and is used for Case I, II and III. The model is one of four models in the paper [1] and requires the largest strength levels among them.

#### Parallel Combination Model

The overall hysteretic model is characterized by changing the strength and displacement levels corresponding to cracking and yielding point of two hysteretic models connected in parallel. The models in Case I and II, and Case III are illustrated in Fig. 7a and b, respectively, but the stiffness  $K_3$  in Case I is different from that in Case II and has no slope. The characteristic parameters of all models are listed in Table 1. Note that each characteristic displacement  $\delta$  corresponds to the mean peak ground acceleration equal to the acceleration of gravity and varies in proportion to the acceleration. The values  $Q_{sc}$  and  $Q_{by}$  are assigned variables on dynamic response analyses and are normalized by the product of the mass and mean peak ground acceleration, changing into  $\beta_S$  and  $\beta_B$ , respectively. These parameters can be considered as the ratio of base shear coefficient to coefficient of the mean peak ground acceleration. Note that the natural period of each model varies in inverse proportion to the square root of its strength level by reason of constant displacement.

It should be recognized that response of a single degree freedom structural system can be applied to estimate response of corresponding multi-degree freedom structural system based on engineering judgement in a case where the latter system behaves in such a type as shown in Fig. 8a and b. Strong-column and weak-girder frame structures are considered to be a typical type shown in Fig. 8b.

#### DUCTILITY RESPONSE

The complete time history of dynamic response was generated for each structural model subjected separately to the twenty artificial earthquake accelerograms of Type B. The response quantity of primary interest is the ductility factors  $\mu_S$  and  $\mu_B$  which are defined as  $\delta(t)_{max}/\delta_{sc}$  and  $\delta(t)_{max}/\delta_{by}$ , respectively. Mean ductility factors and their corresponding coefficients of variation were generated for each model using the twenty response time histories. Ductility factors  $\mu_S$  and  $\mu_B$  for various strength ratios  $\beta_S$  and  $\beta_B$  of each model were computed in probabilistic terms by using the above results. An example is shown in Fig. 9 for Case I-1 at the 85% probability distribution level following the Gumbel Type I distribution of the paper [4].

#### REQUIRED STRENGTH LEVELS

Using data such as shown in Fig. 9 for each case, i.e. using curves of  $\mu_{85}$  vs.  $\beta_B$ , one can easily obtain the required strength ratios  $\beta_B$  of a degrading trilinear model for the required strength ratios  $\beta_S$  of an origin-oriented model.

The resulting required strength ratios  $\beta_B$  can then be plotted as functions of  $\beta_S$  as shown in Fig. 10. The other axes of abscissa and ordinate are expressed in terms of the initial natural periods depending on each of  $\beta_S$  and  $\beta_B$ , respectively. The resulting curves show the interaction effects between the required strength ratios  $\beta_S$  and  $\beta_B$  of both hysteretic models for various levels of ductility factors. The interaction curves obtained in the same manner are shown in Figs. 11 through 18.

The relationship shown in these figures will serve as basic one for wall-frame reinforced concrete buildings to estimate required strength level in seismic design, ductility factor in damage assessment and peak ground acceleration in seismic-capacity evaluation, where two of three parameters, namely, required strength level, ductility factor and peak ground acceleration are previously determined.

#### DISCUSSION OF REQUIRED STRENGTH LEVELS

Required strength ratios of each independent hysteretic model plotted on the axes of abscissa and ordinate can be evaluated by using the results in the paper [1]. For example, the values of  $\beta_B$  for  $\mu_{g5}$  equal to 2, 4, 6 and 8 on the axis of ordinate in Fig. 10 are estimated as the intersecting point of four solid lines and two dotted lines shown in Fig. 3. The dotted line is determined in Eq. 1.

$$T_2 = \sqrt{2} T_1 = 0.2\sqrt{\delta_{by}/\beta_B} \quad (1)$$

where the value of  $\delta_{by}$  equal to 2.25 or 6.75 cm corresponds to  $\ddot{v}_g$  equal to the acceleration of gravity. It might be better to define the period of degrading trilinear models by the value of  $T_2$  as stated in the paper [6] in a case where the models are characterized by the value of  $\delta_{by}$ .

Required strength ratios  $\beta$  are independent of yielding displacement levels  $\delta_y$  in a range of the constant value of  $\beta$  regardless of the periods  $T_1$  as illustrated in Fig. 19. This trend is observed on the nearly constant values of  $\beta_S$  for  $\mu_S$  and  $\mu_B$  in Figs. 10 through 13 and on those of  $\beta_B$  for  $\mu_B$  equal to 2 in Figs. 10, 13 and 14. In observing the Figs. 10 through 18, the values of  $\beta_S$  increase with increasing values of  $\delta_{sc}$ , and the values of  $\beta_B$  decrease with increase values of  $\delta_{by}$ . These trends are explained by the relationship between  $\beta$ ,  $T_1$ ,  $\mu$  and  $\delta$  shown in Figs. 2 and 3.

The interaction curves shown in Figs. 10 through 18 may be approximated by a straight line for all values of  $\mu$  in Case I and Case III, and for the values of  $\mu_S$  (smaller ductility factors) in Case II, giving solid line AB and dotted line CD illustrated in Fig. 20. The interaction curves for the value of  $\mu_B$  in Case II may be approximated by an ellipse as illustrated by solid line CD in Fig. 20. One significant feature shown in Figs. 16, 17 and 18 is that the values of  $\mu_S$  in Case II and III are very close each other in a range where the values of  $\mu_B$  is relatively small. These trends result from the negative slope of the stiffness  $K_3$  and from the different relationship between  $\delta_{sy}$  and  $\delta_{by}$ .

The interaction curves of required strength ratios for parallel combination models will be prepared by using the above-mentioned process. More required strength ratios  $\beta_B$  on the axis of ordinate can be obtained by using the results in the paper [1], where basic data had been prepared for three more degrading trilinear models subjected to five types of artificial earthquake accelerograms.

CONCLUSIVE STATEMENT

The interaction curves of required strength ratios for a parallel combination model idealizing wall-frame reinforced concrete buildings were prepared changing the characteristic parameters of the model and were related to independent required strength ratios of both hysteretic models composing the parallel combination model.

REFERENCES

- [1] Murakami, M. and J. Penzien, "Nonlinear Response Spectra for Probabilistic Seismic Design and Damage Assessment of Reinforced Concrete Structures," Report No. EERC 75-38, University of California, Berkeley, Ca., U.S.A., November 1975.
- [2] Hisano, M. and T. Okada, "Earthquake Response of R/C Frame-Wall Buildings," Proceedings of the A.I.J. Annual Convention, October 1975 (in Japanese).
- [3] Jennings, P.C., et al., "Simulated Earthquake Motions," EERL, California Institute of Technology, Pasadena, Ca., U.S.A., April 1968.
- [4] Gumbel, E. J., and Carlson, P. G., "Extreme Values in Aeronautics," Journal of the Aeronautical Sciences, 21, No. 6, June, 1954.
- [5] Umemura, H., et al., "Earthquake Resistant Design of Reinforced Concrete Buildings, Accounting for the Dynamic Effects of Earthquake," Giho-do, Tokyo, Japan, 1973 (in Japanese).
- [6] Murakami, M. and J. Penzien, "Nonlinear Response Spectra for Probabilistic Seismic Design of Reinforced Concrete Structures," Proceeding of 6th World Conference of Earthquake Engineering, India, January, 1977.

Table 1 Characteristic Parameters of Each Model

	Origin-oriented Model				Degrading Trilinear Model		
	$\delta_{sc}$ (cm)	$\delta_{sy}$ (cm)	$\delta_{sf}$ (cm)	$Q_{sy}/Q_{sc}$	$\delta_{bc}$ (cm)	$\delta_{by}$ (cm)	$Q_{by}/Q_{bc}$
Case I-1	0.075	0.75	-	1.9	0.375	2.25	3.0
Case I-2	0.05	0.5	-	1.9	0.375	2.25	3.0
Case I-3	0.1125	1.125	-	1.9	0.375	2.25	3.0
Case I-4	0.05	0.5	-	1.9	0.25	1.5	3.0
Case I-5	0.1125	1.125	-	1.9	0.5625	3.375	3.0
Case I-6	0.225	2.25	-	1.9	1.125	6.75	3.0
Case II-1	0.075	0.75	2.25	1.9	0.375	2.25	3.0
Case II-2	0.225	2.25	6.75	1.9	1.125	6.75	3.0
Case III	0.375	2.25	6.75	3.0	0.375	2.25	3.0

Notes : relative displacement  $\delta$  is for the mean peak ground acceleration equal to the acceleration of gravity, and varies in proportion to the acceleration.

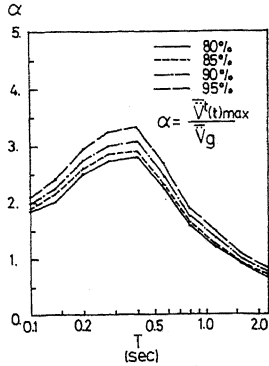


Fig. 1 Required Acceleration Ratios for Linear Model at Four Probability Distribution Levels

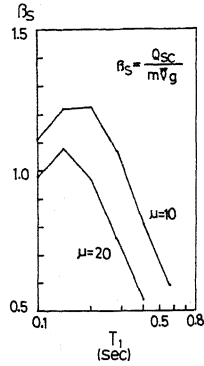


Fig. 2 Required Strength Ratios for Origin-oriented Model at the 85% Probability Distribution Level

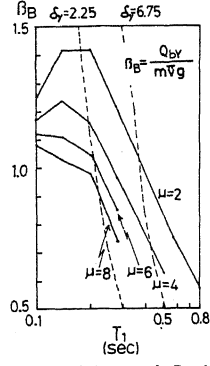


Fig. 3 Required Strength Ratios for Degrading Trilinear Model at the 85% Probability Distribution Level

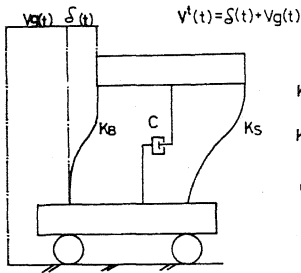


Fig. 4 Single Degree of Freedom Model

$K_S$ : Stiffness Properties of shear failure type  
 $K_B$ : Stiffness Properties of flexural failure type  
 $C = \frac{2(hsk_s(t)^{1.5} + h^2 k_B(t)^2 / \sqrt{K_B}) / m}{k_s(t) + k_B(t)}$

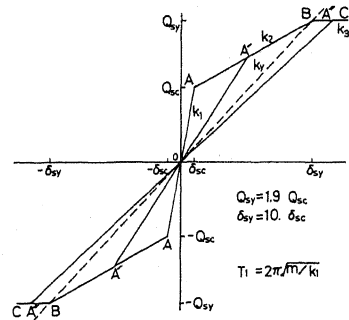


Fig. 5 Origin-oriented Hysteretic Model

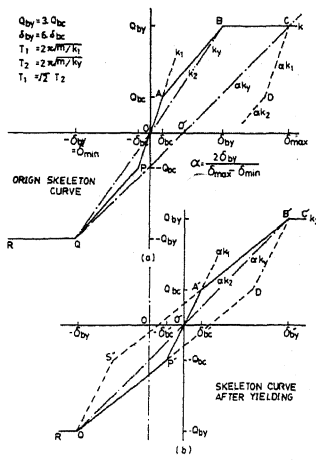


Fig. 6 Degrading Trilinear Hysteretic Model

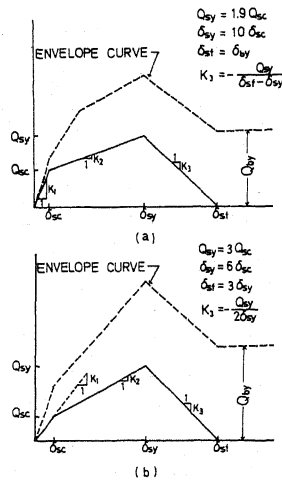


Fig. 7 Skeleton and Envelope Curves for Each Model

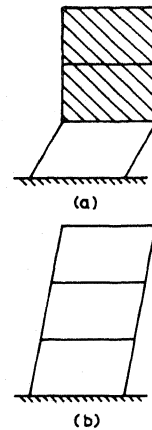


Fig. 8 Idealized Model for Applicative Use

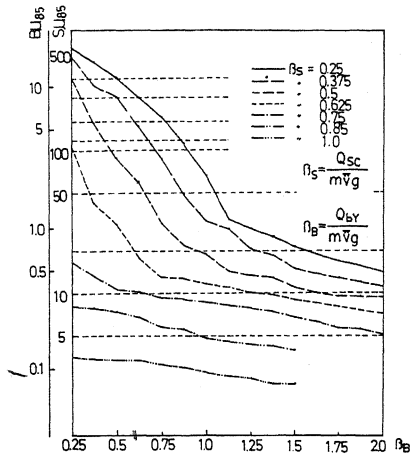


Fig. 9 Response Ductility Factors for Parallel System at the 85% Probability Distribution Level

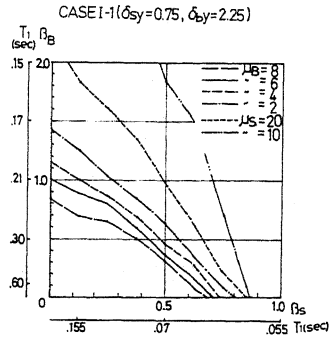


Fig. 10 Interaction Curves of Required Strength Ratios for Case I-1

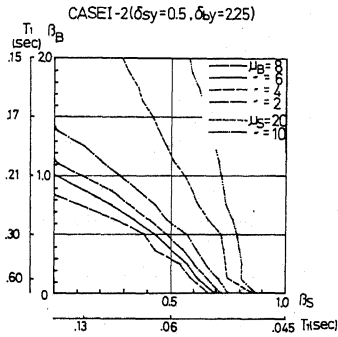


Fig. 11 Interaction Curves of Required Strength Ratios for Case I-2

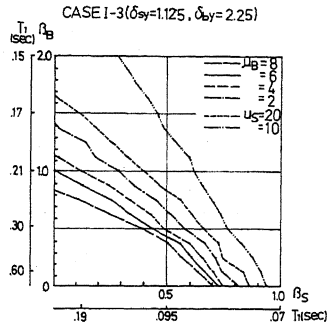


Fig. 12 Interaction Curves of Required Strength Ratios for Case I-3

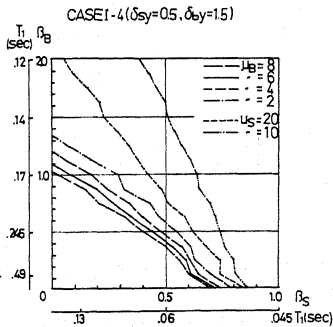


Fig. 13 Interaction Curves of Required Strength Ratios for Case I-4

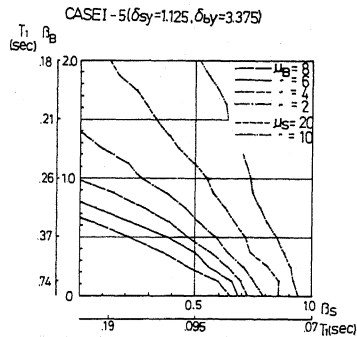


Fig. 14 Interaction Curves of Required Strength Ratios for Case I-5

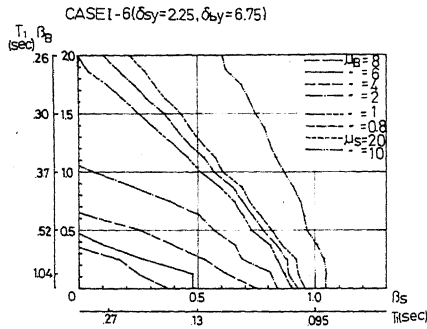


Fig.15 Interaction Curves of Required Strength Ratios for Case I-6

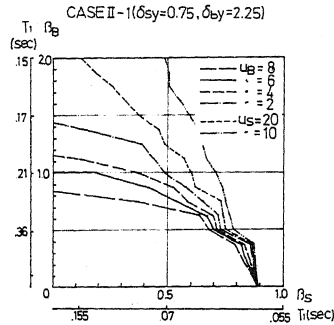


Fig.16 Interaction Curves of Required Strength Ratios for Case II-1

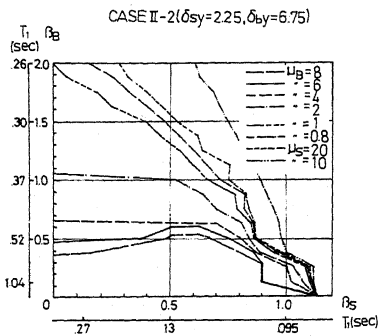


Fig.17 Interaction Curves of Required Strength Ratios for Case II-2

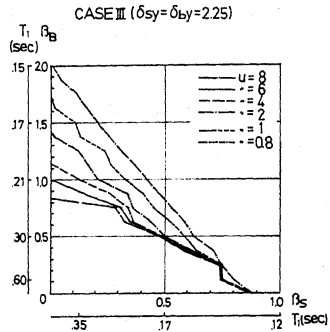


Fig.18 Interaction Curves of Required Strength Ratios for Case III

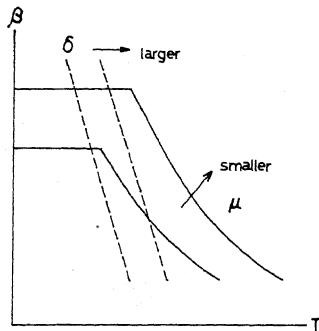


Fig.19 Relationship between Required Strength Levels, Natural Periods, Ductility Factors and Yielding Displacement Levels

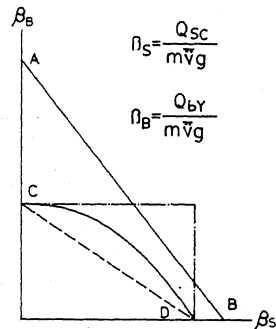


Fig.20 Idealized Interaction Curves of Required Strength Ratios